AXISYMMETRIC MAGNETIC FIELD CALCULATION WITH ZONAL HARMONIC EXPANSION

F. Glück[1, 2, *]

[1]Karlsruhe Institute of Technology, IEKP, 76021 Karlsruhe, P. O. Box 3640, Germany

[2]KFKI, RMKI, H-1525 Budapest, P. O. Box 49, Hungary

Abstract—The magnetic field of an axially symmetric coil or magnetic material system can be computed by expansion of the central and remote zonal harmonics, using the Legendre polynomials. This method can be 100–1000 times faster than the more widely known elliptic integral method and is more general than the similar radial series expansion. We present the zonal harmonic method for field, scalar and vector potential calculation of circular current loops, of general axisymmetric coils and magnetic materials, and of special coils with rectangular cross section, with various source representations: currents, magnetic dipoles and equivalent magnetic charges. We discuss in detail the convergence properties of the zonal harmonic expansions, and we show the generalization of the method for special three-dimensional magnetic systems.

1. INTRODUCTION

Axisymmetric magnetic field calculation is important in many areas of physics: electron and ion optics, charged particle beams, charged particle trapping, electron microscopy, electron spectroscopy, plasma and ion sources, electron guns, etc. [1–3]. Magnetic field calculations are needed for the optimal design of various kinds of uncooled, water-cooled and superconducting coils [4]. An important application of axially symmetric superconducting coils with high homogeneity and efficient shielding requirements is nuclear magnetic resonance for medical imaging [5–10]. On the fundamental physics side, a special kind of electron and ion energy spectroscopy is realized by the MAC-E filter spectrometers, where integral energy spectrum is

measured by the combination of electrostatic retardation and magnetic adiabatic collimation. Examples are: the Mainz and Troitsk electron spectrometers [11, 12], the aSPECT proton spectrometer [13, 14], the WITCH ion spectrometer [15, 16], and the KATRIN pre- and main electron spectrometers [17].

It has been known for a long time [18–22] that axisymmetric electric and magnetic fields can be calculated by zonal harmonic expansion. Garrett showed in several papers [23–26] that in the case of axisymmetric magnetic systems the zonal harmonic expansion method has several practical advantages relative to the more widely known elliptic integral method [27]. The main advantage is the speed: the zonal harmonic method is in some cases 100 or even 1000 times faster than the computation with elliptic integrals. In addition, the lowest order terms in the zonal harmonic series can be helpful for system design, for example to improve the homogeneity of the field or to decrease the stray field with some appropriate shielding method. With the zonal harmonic series one can also easily obtain higher derivatives of the fields. Disadvantages of the zonal harmonic method are: the mathematics is quite sophisticated, and the series are not everywhere convergent. Nevertheless, we shall show in our paper that there is only a rather small volume near the two end regions of a coil where the zonal harmonic method cannot be applied; in a large region the series are convergent, and the rate of convergence is rather high.

Several authors applied Garrett's zonal harmonic method for coil design optimization [4, 28–31]. Nevertheless, one cannot say that the method is widely known in the literature. For example, in many electron optics textbooks the method is not even mentioned, although most of these books investigate in detail the radial series expansion method, which is a special and less efficient version of the zonal harmonic expansion method. The main purpose of our paper is to present a thorough overview of the zonal harmonic expansion method for axisymmetric magnetic field calculations, in order to convince the reader that it is superior to the better known elliptic integral and radial series methods. Using the properties of the Legendre polynomials and the derivatives of the zonal harmonics (summarized in the Appendices A and B of Ref. [32]), we derive and prove in our paper the most important formulas that are necessary to apply the zonal harmonic expansion method for magnetic field computations. We have made some important improvements to Garrett's original computational algorithms, and we extended the application of the method from coils to magnetic materials, from currents to equivalent magnetic charges, and from axisymmetric to special three-dimensional coil systems where each coil is axisymmetric in its local coordinate

system.

The zonal harmonic expansion method is very fast and accurate, and these features make it ideal for high precision and long time trajectory computations. Using this method, the magnetic field can be computed during the particle tracking 'on-line', i.e., no two-dimensional interpolation grid has to be calculated prior to the tracking; only the one-dimensional source point grid, containing the source constants at the source points, has to be computed in advance. If one insists on using the interpolation method for the tracking simulations, then the computation of the interpolation grid is much faster with the zonal harmonic method than with elliptic integrals.

Based upon a radial series expansion method of axisymmetric magnetic field calculation, developed by us for electromagnetic design simulations of the aSPECT experiment [13, 14], the C code Bfield_3D was written at the University of Mainz [33] and applied for various magnetic field simulations of the Mainz neutrino mass spectrometer and the KATRIN experiment [33–36]. To apply the zonal harmonic method for magnetic field computations, we have written several FORTRAN and C codes that have been used for electromagnetic design studies and/or trajectory calculations connected with the aSPECT proton spectrometer [13], the Mainz neutrino mass spectrometer [11, 37], the WITCH ion spectrometer [16], the Nab neutron decay spectrometer [38], the PERC neutron decay channel [39], and the KATRIN experiment [17, 40–52]. Note that all the diploma theses and dissertations cited in our paper can be found either on the KATRIN homepage [53] or on the working group homepage of Weinheimer [54]. Based upon our algorithms and C codes, further magnetic field simulation C and C++ codes have been written at the University of Münster [55], at MIT [56], and at KIT [57]. The zonal harmonic method presented in this paper has been included into the C++ simulation package KASSIOPEIA of the KATRIN experiment [58].

The plan of our paper is the following. In Section 2, we introduce the notions source point, central and remote regions, and source constants, we present the central and remote zonal harmonic expansion formulas for magnetic field, scalar and vector potential calculation, and we compare them with the radial series expansion formulas. Sections 3 through 6 contain formulas of source constants for current loops, for general axisymmetric coils, for general magnetic materials, and for coils with rectangular cross section. We present also the derivations of these formulas, with test calculations and connections among the various formulas. Note that all the field expansion and source constant formulas in our paper have been tested by comparisons with our

computer codes. Section 5 contains also some considerations about the equivalent current and magnetic charge models of magnetic materials, and in Section 6 we extend the electric current simulation method of coils with the magnetic charge method. In Section 7, we present some considerations about convergence properties of the zonal harmonic series, and we give numerical examples for the convergence rates of various magnetic systems. In Section 8, we show that the zonal harmonic method can also be applied for field computation of three-dimensional magnetic systems where all coils or magnetic materials are axially symmetric in some local coordinate system. Finally, in Section 9, we give some practical advice about using the zonal harmonic expansion method, and we present computation time values for some special field calculations of coils.

2. ZONAL HARMONIC MAGNETIC FIELD EXPANSION

Let us assume that the magnetic system (consisting of coils and magnetic materials) is axially symmetric relative to the symmetry axis z. This means: the current has only an azimuthal component, the magnetization has only axial and radial components, and both are independent of the azimuthal angle.

Let us define an arbitrary reference point on the symmetry axis, with axial coordinate z_0; we call it a source point. An arbitrary point
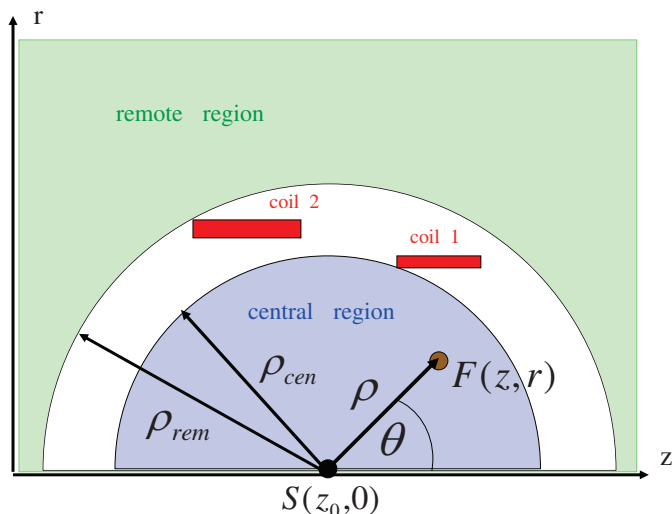
Figure 1. Coils c1 and c2, with field point F, source point S, and with the central ($\rho < \rho_{cen}$) and remote ($\rho > \rho_{rem}$) convergence regions.

where we want to calculate the magnetic field will be called a field point; it has the Descartes coordinates x, y, z. This field point (denoted by F in Fig. 1) can be defined by the cylindrical coordinates z and r (where $r = \sqrt{x^2 + y^2}$), or by the distance ρ between the source point and the field point, and by the angle θ between the symmetry axis z and the direction vector connecting the source and field points:

$$\rho = \sqrt{(z - z_0)^2 + r^2}, \quad u = \cos\theta = (z - z_0)/\rho,$$
$$s = \sin\theta = \sqrt{1 - u^2} = r/\rho \tag{1}$$

(due to the axial symmetry, the azimuthal angle of the field point is not relevant).

We assume that the magnetic system is constrained inside a spherical shell with the source point $S(z_0, 0)$ as center: there is no current and magnetization inside the sphere with center S and radius ρ_{cen} and outside the sphere with center S and radius ρ_{rem}. The central and remote convergence radius ρ_{cen} and ρ_{rem} are the minimal and maximal distances between the source point and the magnetic sources (currents and magnetization), respectively. We call the area $\rho < \rho_{cen}$ central region and the area $\rho > \rho_{rem}$ remote region. Fig. 1 shows an example with 2 coils.

Inside a source-free region, the magnetic scalar potential satisfies the Laplace equation and can be generally written as an expansion of spherical harmonics. In the special case of axial symmetry the spherical harmonics are restricted to the zonal harmonics: $\rho^n P_n(u)$ in the central region and $\rho^{-(n+1)} P_n(u)$ in the remote region, with $P_n(u)$ being the Legendre polynomial of order n.

2.1. Central Region

In the central region, we get the following expansion formulas for the axial and radial magnetic field components B_z and B_r, the magnetic scalar potential V, and the azimuthal component $A = A_\phi$ of the vector potential (all of them depend on the cylindrical coordinates z and r):

$$B_z = \sum_{n=0}^{\infty} B_n^{cen} \left(\frac{\rho}{\rho_{cen}}\right)^n P_n(u), \tag{2}$$

$$B_r = -s \sum_{n=1}^{\infty} \frac{B_n^{cen}}{n+1} \left(\frac{\rho}{\rho_{cen}}\right)^n P_n'(u), \tag{3}$$

$$V = V_0(z_0) - \frac{\rho_{cen}}{\mu_0} \sum_{n=1}^{\infty} \frac{B_{n-1}^{cen}}{n} \left(\frac{\rho}{\rho_{cen}}\right)^n P_n(u), \tag{4}$$

$$A = s\rho_{cen} \sum_{n=1}^{\infty} \frac{B_{n-1}^{cen}}{n(n+1)} \left(\frac{\rho}{\rho_{cen}}\right)^n P_n'(u), \tag{5}$$

where $P_n'(u) = dP_n(u)/du$ denotes the first derivative of the Legendre polynomial of order n, and the magnetic scalar potential at the source point can be computed by integrating the axial magnetic field $B_0(z) = B_z(z,0)$:

$$V_0(z_0) = \frac{1}{\mu_0} \int_{z_0}^{\infty} dz' \, B_0(z'). \tag{6}$$

In order to compute the $P_n(u)$ and $P_n'(u)$ values for very high indices n, one can use the recurrence relations (A11) and (A12) of Ref. [32].

Using Eqs. (A20)–(A28) and (B1)–(B8) in Appendices A and B of Ref. [32], we have checked that the above formulas satisfy the fundamental static magnetic field equations in vacuum: $\Delta V = 0$, $\nabla \cdot \mathbf{B} = 0$, $\nabla \times \mathbf{B} = 0$, $\mathbf{B} = -\mu_0 \nabla V = \nabla \times \mathbf{A}$. Eq. (4) can be useful for some computer programs (like SIMION) that need the magnetic scalar potential as an input for the magnetic field calculation. The vector potential of Eq. (5) can be used to derive or to check the magnetic field lines of the axisymmetric system and to compute the axial angular momentum of a charged particle; in axisymmetric fields this is an invariant quantity, like the energy (see Ref. [3]).

We have defined the coefficients B_n^{cen} ($n = 0, 1, \ldots$) so that each of them has the dimension of the magnetic induction field $\mathbf{B}$, and B_0^{cen} is equal to the axial magnetic field at the source point z_0. We shall call these coefficients central source constants: they represent inside the central region the magnetic field sources (coils and magnetic materials). They depend on the magnetic sources and on the given source point: $B_n^{cen} = B_n^{cen}(z_0)$; in Sections 3, 4 and 5, we present central source constant formulas for various kinds of magnetic sources (with derivations). In the present section, we show some general properties of the source constants. First, the central source constants B_n^{cen} are proportional to the higher derivatives of the on-axis magnetic field function $B_0(z)$ at the source point z_0. In order to understand this relation, let us take a special field point on the axis ($r = 0$) with $z > z_0$. Then $\theta = 0$, $u = 1$, $P_n(1) = 1$, $\rho = z - z_0$, therefore from Eq. (2), we get

$$B_z(z,0) = B_0(z) = \sum_{n=0}^{\infty} B_n^{cen} \frac{1}{\rho_{cen}^n} (z - z_0)^n. \tag{7}$$

Comparing this equation with the general Taylor expansion formula of

the on-axis magnetic field $B_0(z)$ around the source point z_0

$$B_0(z) = \sum_{n=0}^{\infty} \frac{1}{n!} \frac{d^n B_0}{dz^n}(z_0)(z - z_0)^n, \tag{8}$$

we get the relation:

$$B_n^{cen} = B_n^{cen}(z_0) = \frac{\rho_{cen}^n}{n!} \frac{d^n B_0}{dz^n}(z_0). \tag{9}$$

Using this formula, we can express the first z_0-derivative of B_n^{cen} with another central source constant:

$$\partial_{z_0} B_n^{cen} = \frac{n+1}{\rho_{cen}} B_{n+1}^{cen}. \tag{10}$$

This equation will be used later to calculate central source constants for some special cases.

The central zonal harmonic expansions of Eqs. (2)–(5) are convergent only for $\rho < \rho_{cen}$. The convergence is fast if the convergence ratio $\rho/\rho_{cen} \ll 1$, and rather slow if ρ is close to ρ_{cen} (in this case many terms have to be evaluated, in order to get a prescribed accuracy). For $\rho > \rho_{cen}$ the above expansions should not be used, because they provide then meaningless results, due to their divergence.

2.2. Radial Series Expansion

It is well known in electron optics that for an axially symmetric magnetic system the off-axis magnetic field is completely determined by the on-axis potential if the field point is not far from the symmetry axis. The off-axis magnetic field can be expressed by the radial series expansion, which contains the higher derivatives of the on-axis field [1–3]. This expansion is a special case of the more general zonal harmonic expansion. Namely, in the case of the radial series expansion the field point and the source point have the same axial coordinate values: $z = z_0$. That means: $\theta = 90°$ (the line connecting the field and source points is perpendicular to the z axis), $u = 0$ and $\rho = r$. Using Eq. (A5) in Ref. [32], and the connection between the central source constants and the higher derivatives $d^n B_0/dz^n$ in Eq. (9), we obtain

$$B_z(z, r) = \sum_{n=0}^{\infty} \frac{(-1)^n}{(2^n n!)^2} \frac{d^{2n} B_0}{dz^{2n}}(z) \, r^{2n} \tag{11}$$

(a similar expression holds for B_r). This is the radial series expansion that is presented in most electron optics books [1–3]. Similarly to the central zonal harmonic expansion, Eq. (11) is convergent only for $r < \rho_{cen}$. With the knowledge of the higher derivatives or of

the central source constants at the source point z_0, the radial series expansion makes possible the calculation of the potential and field at points of the 2-dimensional plane $z = z_0$ (which is perpendicular to the z axis, going through the point z_0). On the other hand, using the zonal harmonic expansion, the field calculation is possible within a 3-dimensional region ($\rho < \rho_{cen}$). Changing the z coordinate of the field point, one needs different source constants for the radial series expansion, since for this calculation method the field point and the source point should have the same axial coordinate values. In the case of the zonal harmonic expansion this complication is not present: one can use the same central source constants for all field points which are inside the convergence sphere with radius ρ_{cen} and center $z = z_0$, $r = 0$.

2.3. Minimal and Effective Central Region

The central convergence radius ρ_{cen} is, in general, the minimal distance between the source point and the magnetic sources (currents and magnetic dipoles):

$$\rho_{cen} = \rho_{cen}^{\min} = \min_{Z,R} \sqrt{R^2 + (Z - z_0)^2}, \tag{12}$$

where Z and R denote the cylindrical coordinates of an arbitrary point of the coil or magnetic material (we use this notation throughout the paper). We call $\rho_{cen}^{\min}$ a minimal central convergence radius and the $\rho < \rho_{cen}^{\min}$ area a minimal central region.

In special cases, however, one can define a larger central convergence region. Namely, if the current density or magnetization has no Z-dependence, one can perform an analytical integration in the source constant formulas over Z, and it turns out that in this case the central zonal harmonic expansions (2)–(5) converge within a sphere having the radius

$$\rho_{cen} = \rho_{cen}^{eff} = \min_R \left\{ \sqrt{R^2 + (Z_{\min}(R) - z_0)^2}, \sqrt{R^2 + (Z_{\max}(R) - z_0)^2} \right\}, \tag{13}$$

i.e., the central convergence radius is then the minimal distance of the source point from the axial boundary points $Z_{\min}(R)$ and $Z_{\max}(R)$ of the analytical integrals over Z. Fig. 2 shows an example for a coil with rectangular cross section and Z-independent current density. The effective central region having the radius ρ_{cen}^{eff} can be substantially larger than the minimal central region (especially for a long coil whose length is much larger than its radius), i.e., one can then apply the fast zonal harmonic expansion method in a much larger region of field points. However, in contrast to the minimal central region, the effective central region is not free from magnetic sources, therefore Eqs. (2)–(5),
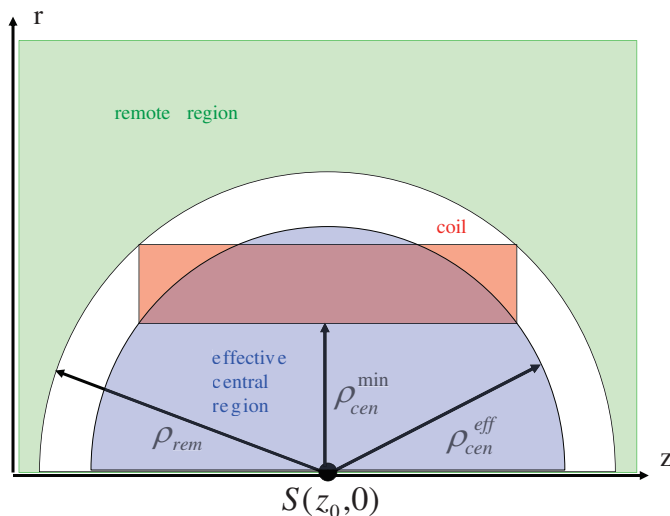
Figure 2. The effective central region for a coil with Z-independent current density.

which are valid only in vacuum, need some correction terms to apply them within the whole effective central region. Such correction terms for a coil with rectangular cross section can be found in Section 6. A detailed discussion about the convergence properties of the central zonal harmonic expansions is in Section 6 of Ref. [32].

To have a better understanding of the effective central region of a coil with constant or Z-independent current density (Fig. 2), we can replace the coil as a superposition of an infinitely long coil without axial boundaries and of 2 infinitely long coils with axial regions $(-\infty, Z_{\min})$ and $(Z_{\max}, \infty)$. The coil without axial boundaries has, by symmetry arguments, constant axial magnetic field, thus its central source constants are zero for $n > 0$, and the minimal central convergence radius of the other two coils is obviously the ρ_{cen}^{eff} value defined by Eq. (13).

2.4. Remote Region

In the remote region $(\rho > \rho_{rem})$ we get the following remote zonal harmonic expansion formulas:

$$B_z = \sum_{n=2}^{\infty} B_n^{rem} \left(\frac{\rho_{rem}}{\rho} \right)^{n+1} P_n(u), \qquad (14)$$

$$B_r = s \sum_{n=2}^{\infty} \frac{B_n^{rem}}{n} \left(\frac{\rho_{rem}}{\rho} \right)^{n+1} P_n'(u), \tag{15}$$

$$V = V_0(\pm\infty) + \frac{\rho_{rem}}{\mu_0} \sum_{n=1}^{\infty} \frac{B_{n+1}^{rem}}{n+1} \left(\frac{\rho_{rem}}{\rho} \right)^{n+1} P_n(u), \tag{16}$$

$$A = s\rho_{rem} \sum_{n=1}^{\infty} \frac{B_{n+1}^{rem}}{n(n+1)} \left(\frac{\rho_{rem}}{\rho} \right)^{n+1} P_n'(u), \tag{17}$$

where $V_0(\pm\infty)$ is zero for $z > z_0$, and it is equal to the total ampere-turn of the system for $z < z_0$. Using Eqs. (A20)–(A28) and (B1)–(B8) in Appendices A and B of Ref. [32], we have checked that the above formulas satisfy the fundamental static magnetic field equations in vacuum: $\Delta V = 0$, $\nabla \cdot \mathbf{B} = 0$, $\nabla \times \mathbf{B} = 0$, $\mathbf{B} = -\mu_0 \nabla V = \nabla \times \mathbf{A}$.

The remote convergence radius ρ_{rem} is the maximal distance between the source point and the magnetic sources (currents and magnetic materials). This is the same as the maximal distance between the source point and the axial boundary points $Z_{\min}(R)$ and $Z_{\max}(R)$, therefore in this case the effective and the normal remote regions are identical.

The coefficients B_n^{rem} ($n = 2, 3, \ldots$) are the remote source constants: they represent in the remote region the magnetic field sources (coils and magnetic materials). They depend on the magnetic sources and on the given source point: $B_n^{rem} = B_n^{rem}(z_0)$; in Sections 3, 4, 5 and 6, we present remote source constant formulas for various kinds of magnetic sources (with derivations).

The above remote zonal harmonic expansions correspond to the multipole expansion of magnetic field for axisymmetric systems: the first term in each equation corresponds to the magnetic dipole, the second to the quadrupole, etc.. The remote source constants B_n^{rem} are proportional to the multipole magnetic moments. For example

$$B_2^{rem} = \frac{\mu_0}{2\pi \rho_{rem}^3} m_z, \tag{18}$$

where m_z denotes the dipole magnetic moment of the system (in case of axial symmetry only the axial component is non-zero). Using the $n = 2$ terms in Eqs. (14) and (15), and the $n = 1$ terms in Eqs. (16) and (17), together with Eq. (18), we obtain the axisymmetric magnetic dipole formulas (with the notation $k = \mu_0/(4\pi)$):

$$\begin{aligned} B_z &= km_z \frac{3\cos^2\theta - 1}{\rho^3}, \quad B_r = km_z \frac{3\sin\theta\,\cos\theta}{\rho^3}, \\ V &= \frac{m_z}{4\pi} \frac{\cos\theta}{\rho^2}, \qquad\qquad A = km_z \frac{\sin\theta}{\rho^2}. \end{aligned} \tag{19}$$

Note that we use SI units throughout our paper.

The above remote zonal harmonic expansion formulas are convergent only for $\rho > \rho_{rem}$. The convergence is fast if the convergence ratio $\rho_{rem}/\rho \ll 1$, and rather slow if ρ is close to ρ_{rem} (in this case many terms have to be evaluated, in order to get a prescribed accuracy). For $\rho < \rho_{rem}$ the above expansions should not be used, because they provide then meaningless results, due to their divergence.

In special cases the magnetic system is symmetric or antisymmetric relative to the source point. For example, computing the field of a coil that is symmetric to its center, and having the source point at this center, we notice that both the central and the remote source constants have this symmetry, i.e., they are zero for odd n. In this case, one has to use only the even n Legendre polynomial terms for the field calculations, and only the odd n terms for the scalar and vector potential calculations. The alternate recurrence relations of Eqs. (A14)–(A19) in [32] can then help to increase the computation speed.

Within the spherical shell $\rho_{cen} < \rho < \rho_{rem}$ neither the central nor the remote zonal harmonic series are convergent. Nevertheless, the source point z_0 can be arbitrarily chosen on the symmetry axis, and for the various source points we get various central and remote regions. Calculating the source constants for many source points, one can find a large spatial region where either the central or the remote zonal harmonic expansion formulas, for some source point, can be used to calculate the magnetic field. Using the equivalent magnetic charge method for field calculation of a coil (see Section 6), we can extend the zonal harmonic expansion method to a large region where the usual current method is not convergent. At the end, small regions near both ends of a coil remain where one has to use elliptic integrals for the field computations.

2.5. Source Constants and Magnetic Design

The source constants are useful for magnetic system design optimization. In order to obtain a homogeneous field inside a magnetic system, one can compute the central source constants at the center of the volume where we need the good homogeneity, and one can adjust the geometry and currents of the coils and magnetic materials so that the first few central source constants $B_1^{cen}, B_2^{cen}, \ldots$ become zero or small [5, 23, 26]. In case of mirror symmetry the odd n source constants are automatically zero, so the procedure is simpler. To find the optimal configuration with vanishing low-order central source constants, one can write an optimization algorithm (due to practical considerations this has to be often a constrained optimization procedure), but according to our experience, the optimization can

also be performed 'by hand'; of course, one has to start with some meaningful configuration. An example for axisymmetric coil design with high-order homogeneity at two regions can be found in Ref. [13]. Furthermore, to reduce the stray magnetic field of a system, one could search for a configuration where the first few remote source constants $B_2^{rem}, B_3^{rem}, \ldots$ are zero or small (passive or active magnetic shielding).

3. SOURCE CONSTANTS FOR A CIRCULAR CURRENT LOOP

In order to calculate the magnetic field with the zonal harmonic expansion method, we need the source constants. For a fixed source point, these numbers contain the whole information about the sources of the magnetic field. We present in this section the calculation of the central and remote source constants for the simplest axisymmetric current system: the circular current loop.

We use the notations Z, R and I for the axial coordinate, radius and current of the circular current loop, respectively, and we call the point (Z, R) on the cylindrical meridian plane a loop point L. Let us fix on the symmetry axis z a source point S with axial coordinate z_0, and let us denote the distance between the source point S and the loop point L by ρ_s, and the angle between the axis z and the S-L line by θ_s (see Fig. 3). ρ_s and $\cos\theta_s$ can be expressed as

$$\rho_s = \sqrt{(Z - z_0)^2 + R^2}, \quad u_s = \cos\theta_s = (Z - z_0)/\rho_s. \qquad (20)$$

Note that here the loop point L and the source variables Z, R, ρ_s and u_s are analogous to the field point F and the field variables z, r, ρ and u of Section 2.
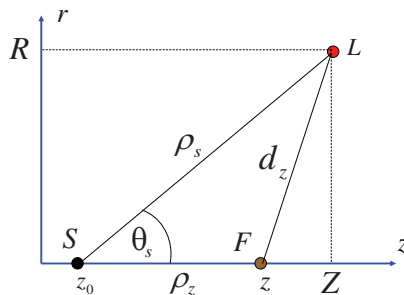
Figure 3. The current loop point L, source point S, axial field point F triangle. Positive current at point L flows out of the page (forming a right-handed screw with the axis z).

Both the central and the remote convergence radii of the loop are equal to ρ_s. Nevertheless, we want to write here the source constant expressions in a general form, so that the current loop could be later considered as part of a more complex magnetic system. Therefore, we assume that $\rho_{cen} \leq \rho_s \leq \rho_{rem}$, i.e., the loop is between the sphere surfaces limiting the central and remote regions.

Let us now consider a special field point F on the axis, with axial coordinate z $(z > z_0)$. The magnetic field at this point due to the current loop is (from the Biot-Savart law)

$$B_0(z) = \frac{\mu_0 I R^2}{2 d_z^3}, \tag{21}$$

where $d_z = \sqrt{R^2 + (z - Z)^2}$ denotes the distance of the axial field point F and the loop point L. The source point, the axial field point and the loop point constitute a triangle with side lengths d_z, ρ_s and $\rho_z = z - z_0$ (see Fig. 3). We can express the d_z distance with the other parameters of this triangle:

$$d_z = \sqrt{\rho_s^2 + \rho_z^2 - 2\rho_s \rho_z u_s}. \tag{22}$$

Let us first assume that the axial field point F is inside the central convergence region: $\rho_z < \rho_{cen}$; since $\rho_{cen} \leq \rho_s$, $\rho_z < \rho_s$ is then also valid. Defining $h = \rho_z/\rho_s$, and using the differentiated generating function formula (A9) of Ref. [32], the $1/d_z^3$ factor of Eq. (21) can be written in terms of a Legendre polynomial expansion as follows:

$$\frac{1}{d_z^3} = \frac{1}{\rho_s^3} \sum_{n=0}^{\infty} h^n P'_{n+1}(u_s). \tag{23}$$

Next, let us consider an axial field point F inside the remote convergence region: $\rho_z > \rho_{rem}$; since $\rho_{rem} \geq \rho_s$, $\rho_z > \rho_s$ is then also valid. In this case, we define $h = \rho_s/\rho_z$, and we get the following expansion:

$$\frac{1}{d_z^3} = \frac{1}{\rho_z^3} \sum_{n=0}^{\infty} h^n P'_{n+1}(u_s). \tag{24}$$

Inserting Eqs. (23) and (24) into Eq. (21), and comparing with the $u = P_n(u) = 1$ special version of Eqs. (2) and (14), we get the central and remote source constants of the current loop:

$$B_n^{cen} = \frac{\mu_0 I R^2}{2\rho_s^3} \left(\frac{\rho_{cen}}{\rho_s} \right)^n P'_{n+1}(u_s), \tag{25}$$

$$B_n^{rem} = \frac{\mu_0 I R^2}{2\rho_{rem}^3} \left(\frac{\rho_s}{\rho_{rem}} \right)^{n-2} P'_{n-1}(u_s). \tag{26}$$

In these expressions the current is positive if its direction forms a right-handed screw with the symmetry axis z.

The lowest order central source constant B_0^{cen} is the magnetic field at the source point (compare with Eq. (21) for $\rho_z = 0$). Taking the $n = 2$ term in Eq. (26), and using the $m_z = I\pi R^2$ magnetic dipole moment formula of the circular current loop, we can check that in this special case relation 18 is really valid.

If the magnetic system consists of only one loop, then $\rho_{cen} = \rho_{rem} = \rho_s$, so the n-dependence of the source constants follows the behavior of the first derivative of the Legendre polynomials, i.e., they increase slightly with n (see the asymptotic formula (A8) in Ref. [32]). If the magnetic system consists of many current loops, the source constants of the whole system can be obtained by summing the above expressions for all loops. The source constants for large n are dominated by those loops that are near the boundary of the central or remote region. The contribution of the loops that are far from these boundaries decreases exponentially with increasing n. This means that for a complicated magnetic system the source constants decrease faster than for one loop, hence the rate of convergence of the zonal harmonic expansions (2)–(5), (14)–(17) for a complex system is always faster than for a simple system consisting of only one loop (see Section 7 for further details about convergence properties).

4. SOURCE CONSTANTS FOR A GENERAL AXISYMMETRIC COIL

The circular current loop results can be used to derive the source constants for a general axisymmetric coil. The central source constants can be written as the following two-dimensional integrals on the cylindrical meridian plane:

$$B_n^{cen} = \int\limits_{R_{\min}}^{R_{\max}} dR \int\limits_{Z_{\min}(R)}^{Z_{\max}(R)} dZ \cdot b_n^{cen}(Z, R), \qquad (27)$$

$$b_n^{cen}(Z, R) = \frac{\mu_0\, J\, R^2}{2\rho_s^3} \left(\frac{\rho_{cen}}{\rho_s}\right)^n P_{n+1}'(u_s), \qquad (28)$$

where $J = J(Z, R)$ denotes the azimuthal component of the current density vector $\mathbf{J}$ (the components J_z and J_r are assumed to be zero), $Z_{\min}(R)$ and $Z_{\max}(R)$ are the axial boundaries of the coil for fixed radius R, and $R_{\min}$ and $R_{\max}$ are the radial boundaries of the coil. ρ_s and u_s are defined by Eq. (20).

Similar expressions hold for the remote source constants:

$$B_n^{rem} = \int\limits_{R_{\min}}^{R_{\max}} dR \int\limits_{Z_{\min}(R)}^{Z_{\max}(R)} dZ \cdot b_n^{rem}(Z, R), \qquad (29)$$

$$b_n^{rem}(Z, R) = \frac{\mu_0 \, J \, R^2}{2\rho_{rem}^3} \left(\frac{\rho_s}{\rho_{rem}} \right)^{n-2} P_{n-1}'(u_s). \qquad (30)$$

If the current density is independent of the axial coordinate ($J = J(R)$), the integrations over Z in the above formulas can be carried out analytically. Namely, in this case the following derivative relations are valid:

$$\partial_Z b_{n-1}^{cen} = -\frac{n}{\rho_{cen}} \, b_n^{cen}, \qquad (31)$$

$$\partial_Z b_{n+1}^{rem} = \frac{n+1}{\rho_{rem}} \, b_n^{rem}. \qquad (32)$$

Eq. (31) follows from the general relation (10), because $\partial_Z = -\partial_{z_0}$. It can also be derived from Eq. (18) of Ref. [23], or using Eq. (B7) of Ref. [32]. Eq. (32) follows from Eq. (B5) of Ref. [32].

Therefore, for Z-independent current density we get from these formulas the analytical integrals over the axial variable Z:

$$B_n^{cen} = -\frac{\rho_{cen}}{n} \int\limits_{R_{\min}}^{R_{\max}} dR \cdot \left[b_{n-1}^{cen}(Z, R) \right]_{Z_{\min}(R)}^{Z_{\max}(R)}, \qquad (33)$$

$$B_n^{rem} = \frac{\rho_{rem}}{n+1} \int\limits_{R_{\min}}^{R_{\max}} dR \cdot \left[b_{n+1}^{rem}(Z, R) \right]_{Z_{\min}(R)}^{Z_{\max}(R)}, \qquad (34)$$

where we use the general notation $[f(Z, R)]_a^b = f(b, R) - f(a, R)$.

Equation (33) cannot be used for $n = 0$. But for the case of Z-independent current density the formula $b_0^{cen}(Z, R)$ can also be integrated analytically over Z:

$$B_0^{cen} = \frac{\mu_0}{2} \int\limits_{R_{\min}}^{R_{\max}} dR \cdot \left[J(R) \, u_s \right]_{Z_{\min}(R)}^{Z_{\max}(R)}. \qquad (35)$$

We mention that Appendix C of Ref. [32] contains a simple and accurate one-dimensional numerical integration method, based on 10th order equidistant Lagrange interpolation.

5. SOURCE CONSTANTS FOR AXISYMMETRIC MAGNETIC MATERIAL

Let us denote the axial and radial coordinates of an arbitrary point of the magnetic material by Z and R. The axisymmetric magnetic material has axial and radial magnetization components: $M_z = M_z(Z, R)$, $M_r = M_r(Z, R)$. Similarly to the previous sections, we derive the source constants of the magnetic material from the on-axis magnetic field of a magnetized ring. Let us consider first a small rectangle on the (z, r) meridian plane with axial coordinates Z and $Z + dZ$ and with radial coordinates R and $R + dR$, where dZ and dR are infinitesimally small; this rectangle defines a magnetized ring. The on-axis magnetic field of this ring can be written as

$$B_0(z) = \frac{\mu_0}{2} R dZ dR \left[M_z \partial_z^2 \left(\frac{1}{d_z} \right) + M_r R \, \partial_z \left(\frac{1}{d_z^3} \right) \right], \qquad (36)$$

where $d_z = \sqrt{R^2 + (z - Z)^2}$ denotes the distance of the on-axis point $(z, 0)$ from the ring.

To derive the central source constants corresponding to an arbitrary source point z_0, we assume first that $\rho_z = z - z_0 < \rho_s$, where ρ_s is the distance of the source point z_0 from the magnetized ring (see Eq. (20)). Defining $h = \rho_z/\rho_s$ and writing $d_z = \rho_s\sqrt{1 + h^2 - 2hu_s}$ (see Eq. (22)), we can write the derivative expressions in the above equation as z-derivatives of Legendre polynomial expansions, using Eqs. (A1) and (A9) of Ref. [32]. Comparing these expansions with the on-axis ($u = P_n(u) = 1$, $\rho = \rho_z$) version of Eq. (2), we get the central source constants for the magnetized ring.

To get the remote source constants, we take $\rho_z = z - z_0 > \rho_s$, and we define $h = \rho_s/\rho_z$. Using the above Legendre polynomial expansions and comparing with the on-axis version of Eq. (14), we get the remote source constants for the magnetized ring.

For a general axisymmetric magnetic material system, the central and remote source constants can be expressed by the following two-dimensional integrals:

$$\begin{aligned} B_n^{cen} = &\frac{\mu_0(n+1)}{2} \int dR \int dZ \cdot \frac{R}{\rho_s^3} \left(\frac{\rho_{cen}}{\rho_s} \right)^n \\ &\left[M_z(n+2)P_{n+2}(u_s) + M_r \frac{R}{\rho_s} P_{n+2}'(u_s) \right], \qquad (37) \end{aligned}$$

$$B_n^{rem} = \frac{\mu_0 n}{2} \int dR \int dZ \cdot \frac{R}{\rho_s^3} \left(\frac{\rho_s}{\rho_{rem}} \right)^{n+1}$$
$$\left[M_z(n-1)P_{n-2}(u_s) - M_r \frac{R}{\rho_s} P'_{n-2}(u_s) \right]. \tag{38}$$

If the magnetization functions M_z and M_r are independent of the axial variable Z, the integration over Z can be carried out analytically:

$$B_n^{cen} = -\frac{\mu_0}{2} \int dR \cdot R$$
$$\left[\left(\frac{\rho_{cen}}{\rho_s} \right)^n \left(M_z \frac{n+1}{\rho_s^2} P_{n+1}(u_s) + M_r \frac{R}{\rho_s^3} P'_{n+1}(u_s) \right) \right]_{Z_{\min}(R)}^{Z_{\max}(R)}, \tag{39}$$

$$B_n^{rem} = \frac{\mu_0}{2} \int dR \cdot R$$
$$\left[\left(\frac{\rho_s}{\rho_{rem}} \right)^{n+1} \left(M_z \frac{n}{\rho_s^2} P_{n-1}(u_s) - M_r \frac{R}{\rho_s^3} P'_{n-1}(u_s) \right) \right]_{Z_{\min}(R)}^{Z_{\max}(R)}, \tag{40}$$

where we use the general notation $[f]_a^b = f(b) - f(a)$. To get Eqs. (39) and (40) from Eqs. (37) and (38), we have used the axial derivative formulas (B1), (B3), (B5), (B7) in Ref. [32].

Note that in the case of the integrated formula (39) the effective central convergence radius is the minimal distance of the source point from the axial boundary points $(Z_{\min}(R), R)$ and $(Z_{\max}(R), R)$. This is usually larger than the minimal distance of the source point from the magnetic material.

We have tested the above formulas by computing the field and the scalar and vector potential of various axisymmetric magnetic materials with 3-dimensional numerical integration of the dipole formulas, and by comparing the results with the zonal harmonic expansions presented in Section 2, where the above expressions for the source constants have been used.

The magnetization distribution **M** is equivalent to the sum of volume current density distribution $\mathbf{J}_m = \nabla \times \mathbf{M}$ and surface current density distribution $\mathbf{K}_m = \mathbf{M} \times \mathbf{n}$, where **n** is the outwardly directed normal vector of the magnetic material surface (see Refs. [59, 60]). Note that this equivalence is valid only for the induction field **B**, but not for the field intensity **H**. Using Eqs. (25) and (26) in Section 3, Eqs. (A27), (A28), (B5)–(B8) in Ref. [32], the axisymmetric rotation formula $(\nabla \times \mathbf{M})_\phi = \partial_Z M_r - \partial_R M_z$, and integration by parts, we have checked that the above source constant formulas indeed satisfy these equivalence relations.

From the point of view of the field intensity $\mathbf{H}$ calculation, the magnetization distribution $\mathbf{M}$ is equivalent to the sum of volume magnetic charge density distribution $\rho_m = -\nabla \cdot \mathbf{M}$ and surface magnetic charge density distribution $\sigma_m = \mathbf{M} \cdot \mathbf{n}$ (see Refs. [20, 59, 60]. This equivalence does not hold for the induction field: due to the general relation $\mathbf{B} = \mu_0(\mathbf{M} + \mathbf{H})$ the induction field of the magnetic material and of the equivalent magnetic charge system differ by the magnetization term $\mu_0\mathbf{M}$; in vacuum, however, the induction fields of the two systems are equal. The volume magnetic charge density satisfies also the $\nabla \cdot \mathbf{H} = \rho_m$, $\Delta V = -\rho_m$ equations, due to $\nabla \cdot \mathbf{B} = 0$. We mention that with our conventions the equivalent magnetic charge has the SI unit of Ampere-meter.

A big advantage of the equivalent magnetic charge model is that the computation is similar to the electric field calculation (see Section 20.4 in Ref. [61]). We can simply get the central and remote zonal harmonic expansion formulas for V, H_z and H_r from Eqs. (2)–(4) and (9)–(11) of Ref. [32] by substituting the letters Φ and E for V and H, respectively. For example, the remote expansions for H_z and H_r can be written as

$$H_z = \frac{1}{\rho_{rem}} \sum_{n=1}^{\infty} V_{n-1}^{rem} \cdot n \left(\frac{\rho_{rem}}{\rho} \right)^{n+1} P_n(u), \qquad (41)$$

$$H_r = \frac{s}{\rho_{rem}} \sum_{n=1}^{\infty} V_{n-1}^{rem} \left(\frac{\rho_{rem}}{\rho} \right)^{n+1} P_n'(u). \qquad (42)$$

To get the central and remote source constants V_n^{cen} and V_n^{rem}, in formulas (18)–(19) and (21)–(22) of Ref. [32], we have to make the replacements $\Phi \to V$, $\varepsilon_0 \to 1$, $Q \to Q_m$, $\sigma \to \sigma_m$, where Q_m and σ_m denote the equivalent magnetic charge and surface magnetic charge density, respectively. The V_n^{cen}, V_n^{rem} magnetic source constants of a magnetic material could also be computed by making the $\Phi_n^{cen} \to V_n^{cen}$, $\Phi_n^{rem} \to V_n^{rem}$, $\varepsilon_0 \to 1$, $\mathcal{P}_z \to M_z$, $\mathcal{P}_r \to M_r$ substitutions in the dielectric formulas (27)–(31) of Ref. [32] (in this case the magnetic charges are not used for the field intensity calculation).

It should be emphasized that the equivalent (fictitious) magnetic charge used in the above computation method is completely different from the magnetic monopole (real magnetic charge): the volume density of the latter satisfies the equation $\nabla \cdot \mathbf{B} = \mu_0 \rho_{\text{monopole}}$, which is an extension of the standard Maxwell equations, while the equivalent magnetic charge, as used above, is merely a mathematical tool within the framework of the standard Maxwell equations (with $\nabla \cdot \mathbf{B} = 0$).

The magnetic field of axisymmetric permanent magnets with axial and radial magnetization is calculated in Refs. [62, 63] by elliptic

integrals. The authors of these papers use both the Coulombian model (with equivalent magnetic charges) and the Amperian model (with equivalent currents).

6. MAGNETIC FIELD OF AN AXISYMMETRIC COIL WITH RECTANGULAR CROSS SECTION

6.1. Source Constant Calculation with Radial Numerical Integration

A practically important special axisymmetric current system is a coil with rectangular cross section on the (Z, R) meridian plane and with Z-independent current density $(J = J(R))$. Let us denote the axial and radial boundaries of the coil by $Z_{\min}$, $Z_{\max}$, $R_{\min}$ and $R_{\max}$ (see Fig. 4). The central and remote source constants of this coil can be expressed by the radial integrals of Eqs. (33)–(35), where $Z_{\min}$ and $Z_{\max}$ are independent of R. If the current density is constant (independent also of R), then even the radial integrals can be carried out analytically [23–25, 64, 65]. Nevertheless, we kept in our method the radial numerical integration, avoiding the analytical one. First, the source constant calculation with this numerical integration turned out to be fast and precise enough. Second, the forward recurrence formulas of the analytical integration presented in the above papers are in some cases numerically unstable. This instability problem can be cured by using the recurrence formulas in backward direction, starting with the largest
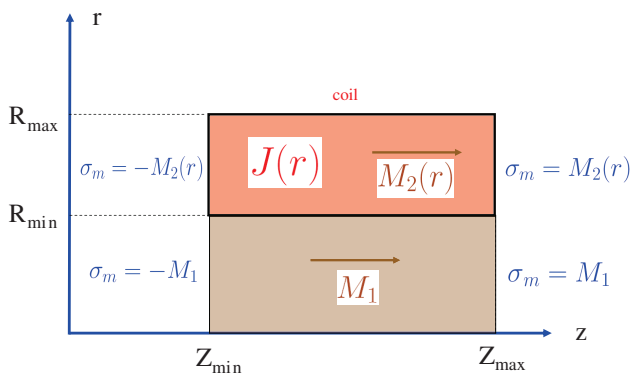
Figure 4. Axisymmetric coil with rectangular cross section in the (z, r) plane and with current density $J(r)$ depending only on the radial coordinate. Equivalent magnetization M_1 and $M_2(r)$, and equivalent magnetic charge density σ_m.

index n. But in this case, one needs a complicated explicit expression for the highest required term (e.g., the term $n_{\max} = 33$ is given in Refs. [24, 25]), therefore the zonal harmonic expansion can be used only up to this $n_{\max}$, and this fact limits the accuracy of the method, especially for field points near the boundaries of the central and remote convergence regions. Using radial numerical integrations (see App. C of Ref. [32] for a simple integration method), the source constants can be computed precisely and with rather short computation time, even for high n values. We mention, though, that the number of integration points necessary to get a satisfactory accuracy for the source constants increases with n and also with the ratio factor $(R_{\max} - R_{\min})/R_{\min}$.

6.2. Correction Term in the Effective Central Region

The central and remote convergence radii of the coil are the minimal and maximal distances of the source point from the 4 corner points of the coil:

$$\rho_{cen} = \min \left[\sqrt{R_{\min}^2 + (Z_{\min} - z_0)^2}, \sqrt{R_{\min}^2 + (Z_{\max} - z_0)^2} \right], \quad (43)$$

$$\rho_{rem} = \max \left[\sqrt{R_{\max}^2 + (Z_{\min} - z_0)^2}, \sqrt{R_{\max}^2 + (Z_{\max} - z_0)^2} \right]. \quad (44)$$

The central convergence radius of Eq. (43) corresponds to the effective central region, introduced in Section 2. For a long coil and a source point near the coil center the effective central region is much larger than the minimal central region, which is defined by the minimal distance of the source point from the coil winding. Therefore, it is expedient to define the central region with Eq. (43). Nevertheless, in this case the central region is not source-free (see Fig. 2), therefore Eqs. (2)–(5) need some additional correction terms. For example, in the effective central region B_z should be calculated by $B_z = B_z[\text{Eq. (2)}] + B_z^{corr}$. To obtain this correction, one has to use the $\nabla \times \mathbf{B} = \mu_0 \mathbf{J}$ Maxwell equation. For axisymmetric coil only the azimuthal components of these vectors are non-zero:

$$(\nabla \times \mathbf{B}^{corr})_\phi = \partial_z B_r^{corr} - \partial_r B_z^{corr} = \mu_0 J(r). \quad (45)$$

The solution of this equation is:

$$B_z^{corr}(r) = -\mu_0 \int\limits_0^r dR \cdot J(R), \qquad B_r^{corr} = 0. \quad (46)$$

Since the current density vanishes for $R < R_{\min}$ and for $R > R_{\max}$, the field correction term is zero for $r < R_{\min}$ and constant for $r > R_{\max}$.

For constant current density the field correction term is simply:

$$
B_z^{corr}(r) = \begin{cases} 0 & : \quad \text{for} \quad r < R_{\min}, \\ -\mu_0 J\left(r - R_{\min}\right) & : \quad \text{for} \quad R_{\min} \leq r \leq R_{\max}, \\ -\mu_0 J\left(R_{\max} - R_{\min}\right) & : \quad \text{for} \quad r > R_{\max}. \end{cases} \quad (47)
$$

The above correction term is non-zero only for $Z_{\min} < z_0 < Z_{\max}$, i.e., if the minimal and the effective central regions are not identical (in this case the effective central region has a common part with the coil winding).

6.3. The Equivalent Magnetic Charge Model

For a given source point, the zonal harmonic expansion method cannot be applied within the spherical shell $\rho_{cen} < \rho < \rho_{rem}$ (see Figs. 1 and 2). There are several methods to reduce this 'forbidden region': by changing the source point position, or by dividing the magnetic system to smaller parts and using a separate source point for each part. For example, in the case of a long coil, one could divide it to smaller subcoils and make separate remote expansions for each subcoil, with source points at the center of each subcoil. Nevertheless, in this case the magnetic field computation time increases with the number of subcoils. We show below that a rather powerful method to improve the application possibilities and speed of the zonal harmonic expansion method is by using equivalent (fictitious) magnetic charges for the field calculation.

We have seen in the previous section that, from the point of view of the B field calculation, a magnetic material can be replaced by an equivalent current system. Vice versa, a coil can also be replaced by equivalent magnetic material that has the same induction field $\mathbf{B}$ as the coil. The coil discussed in the present section can be replaced by an axially magnetized cylinder within the region $Z_{\min} < z < Z_{\max}$, $r < R_{\max}$. Using the equivalent volume current density formula $\mathbf{J} = \nabla \times \mathbf{M}$, the azimuthal component formula $\mathbf{J}_\phi = J(r) = (\nabla \times \mathbf{M})_\phi = -\partial_r M_z$, and the boundary condition requirement $M_z(R_{\max}) = 0$, the equivalent axial magnetization of the coil can be expressed as:

$$
M_z(r) = \begin{cases} M_1 = \int\limits_{R_{\min}}^{R_{\max}} dR \cdot J(R) & : \quad \text{if} \quad r < R_{\min}, \\ M_2(r) = \int\limits_{r}^{R_{\max}} dR \cdot J(R) & : \quad \text{if} \quad R_{\min} \leq r \leq R_{\max}. \end{cases} \quad (48)
$$

If the current density of the coil is constant (J), the integrals above

can be easily calculated analytically:

$$M_z(r) = \begin{cases} M_1 = J \cdot (R_{\max} - R_{\min}) & : \quad \text{if} \quad r < R_{\min}, \\ M_2(r) = J \cdot (R_{\max} - r) & : \quad \text{if} \quad R_{\min} \leq r \leq R_{\max}. \end{cases} \quad (49)$$

With these magnetization formulas and with Eq. (40) we get the same remote source constants as with Eq. (34): for the purpose of magnetic field calculation outside the coil the magnetized cylinder is really equivalent to the coil.

For the central source constants inside the coil the equivalent magnetization is not useful. Nevertheless, we have seen in Section 5 that, as far as the H field is concerned, a magnetic material is equivalent to a magnetically charged system. In our case, the magnetized cylinder corresponding to the coil can be replaced by two magnetically charged disks at the two ends of the coil, both disks having a radius $R_{\max}$. The disk at $z = Z_{\max}$ has an equivalent surface magnetic charge density function $\sigma_m(r) = M_z(r)$, and the disk at $z = Z_{\min}$ has $\sigma_m(r) = -M_z(r)$ (thus the total magnetic charge of the equivalent system is zero). As we have mentioned in Section 5, the H_z and H_r field components and the V_n^{cen} and V_n^{rem} source constants of the magnetically charged disks can be obtained by the $E \to H$, $\Phi \to V$, $\sigma \to \sigma_m$, $\varepsilon_0 \to 1$ substitutions in the electric field formulas of Sections 2 and 4 of Ref. [32]. The $r < R_{\min}$ parts of the disks have constant magnetic charge density $\sigma_m = \sigma_{m1} = \pm M_1$, and according to Section 6 of Ref. [32] the effective central convergence radius of these disk parts is equal to the minimal distance of the source point from the $r = R_{\min}$ disk points. Thus, the equivalent magnetically charged disks have the same effective central convergence region as the coil. Similarly, the remote convergence radius of the 2 disks is the maximal distance between the source point and the $r = R_{\max}$ disk points, and the latter coincide with the outer corner points of the coil. Thus, the two disks and the coil have the same remote convergence regions.

In order to get the B field of the coil from the H field of the disks, the general SI formula

$$\mathbf{B} = \mu_0(\mathbf{M} + \mathbf{H}) \quad (50)$$

should be used, where $\mathbf{M}$ denotes the equivalent axial magnetization of Eqs. (48) and (49) (the radial component of $\mathbf{M}$ is zero). We have tested (both by analytical and numerical calculations) that, using the magnetic charge model together with the above formula, we get the same magnetic induction field of the coil as with the original current model. Note that the discontinuity of the magnetic charge model H field at the disk positions is compensated by the discontinuity of the equivalent axial magnetization, so that the B field is everywhere continuous.
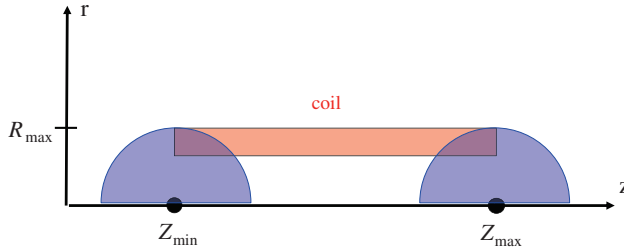
Figure 5. Coil with the two magnetic charge model spheres. The remote expansions of the magnetically charged end-disks of the coil are convergent everywhere outside these spheres.

Using one source point for the H field calculation of the two disks, we realize from the above considerations that the central and remote zonal harmonic expansions of the disks and the coil have the same convergence properties, thus in this case the magnetic charge model has no significant computational advantages compared to the coil calculation presented in Section 4. The situation becomes different if one uses two source points and two separate zonal harmonic expansions, one for each disk. For example, we define the two source points at the axial positions of the disks ($z_0 = Z_{\min}$ and $z_0 = Z_{\max}$), we make two separate remote expansions at these source points, and the field components H_z and H_r at any field point are calculated as the sum of the $H_z^{\min}$, $H_z^{\max}$, $H_r^{\min}$ and $H_r^{\max}$ partial field results of the expansions presented in Eqs. (41) and (42). These remote expansions are convergent at field points outside the two spheres with radii $R_{\max}$ and with the above source points as centers (see Fig. 5). Thus, with the help of the magnetic charge model, the zonal harmonic expansion method can be employed also within a large part of the 'forbidden' zone between the effective central and remote regions (see Fig. 2).

The remote source constants for the above-mentioned remote expansions and for each disk can be expressed as

$$V_n^{rem} = \frac{P_n(0)}{2R_{\max}} \left[\frac{\sigma_{m1} \cdot R_{\max}^2}{n+2} \left(\frac{R_{\min}}{R_{\max}} \right)^{n+2} + \int_{R_{\min}}^{R_{\max}} dR \cdot \sigma_m(R) R \left(\frac{R}{R_{\max}} \right)^n \right].$$

(51)

This formula can be derived from Eq. (22) of [32], using the special values $u_s = 0$, $\rho_s = R$, $\rho_{rem} = R_{\max}$. If the current density of the coil is constant (J), the above integration can be made analytically, and

we get an even simpler formula:

$$V_n^{rem} = \frac{\pm J \cdot P_n(0) \cdot R_{\max}^2}{2(n+2)(n+3)} \left[1 - \left(\frac{R_{\min}}{R_{\max}} \right)^{n+3} \right], \qquad (52)$$

where the + and − signs are for the disks at $z = Z_{\max}$ and $z = Z_{\min}$, respectively. $P_n(0) = 0$ for odd n, thus the remote expansions (41) and (42), using these remote source constants, are twice as fast as the general expansions with non-zero odd and even terms. The $P_n(0)$ values for even n can be simply evaluated by the recurrence relation

$$P_n(0) = -\frac{n-1}{n} P_{n-2}(0), \quad P_0(0) = 1. \qquad (53)$$

The equivalent magnetic charge model is useful to understand some general properties of the coil. It is well known that at the center of a long coil the magnetic field is rather homogeneous. The magnetization part of the B-field is exactly homogeneous for $r < R_{\min}$, and in the case of a long coil the magnetically charged disks are far away from the center, therefore the H-field due to these disks is small: the B-field, dominated by the magnetization part, is nearly homogeneous. Approximating the disks by point charges, we can get a simple quantitative estimate about the inhomogeneity of the field. It is then also obvious that outside the coil ($r > R_{\max}$), where the dominant magnetization part is missing, the B-field is much smaller than inside. Furthermore, near one end of a long coil the H-field of the near disk is much larger than the H-field of the far disk, therefore the magnetic field outside the coil within this region is similar to the field of a magnetic monopole. Finally, the magnetic charge model is also useful for force calculations between coils (see Ref. [66] for force calculation with the usual current method).

7. RATE OF CONVERGENCE

Writing the series of Eqs. (2)–(5) and (14)–(17) generally as $\sum_n c_n x^n$, with $x = \rho/\rho_{cen}$ or $x = \rho_{rem}/\rho$, and assuming that the coefficients c_n have some kind of polynomial n-dependence $c_n \sim n^p$, we can conclude from the Cauchy-Hadamard theorem that all these series are convergent for $x < 1$ and divergent for $x > 1$ (see Section 6 of [32] for more details). According to Eqs. (A7) and (A8) of [32], the Legendre polynomials have $P_n \sim 1/\sqrt{n}$ and $P_n' \sim \sqrt{n}$ asymptotic n-dependence, thus the polynomial n-dependence requirement of the coefficients c_n is equivalent with polynomial n-dependence of the source constants B_n^{cen} and B_n^{rem}. In case of 1 current loop (Section 3) $\rho_{cen} = \rho_{rem} = \rho_s$, and the source constants are proportional to the first derivatives of the

Legendre polynomials (Eqs. (25) and (26)), thus the above requirement is obviously fulfilled. If we have many current loops, and we define ρ_{cen} and ρ_{rem} as the minimal and maximal distance of the source point from the loop points L, respectively (see Fig. 3), the loops closest to the source point (for central series) or farthest from the source point (for remote series) are dominant for the source constant evaluation (the contribution of the other loops decreases exponentially with n), therefore the ratio of the source constants of a general loop system and of 1 loop decreases with n. This implies not only that the zonal harmonic series in the central and remote regions are convergent for a general current loop system, but also that the rate of convergence for a general system is always faster than for 1 loop.

The above definition of ρ_{cen} corresponds to the minimal central convergence radius introduced in Section 2. On the other hand, Eqs. (33), (28) and (39) show us that, in the case of Z-independent current density (for a coil) or Z-independent magnetization (for a magnetic material), the central source constants B_n^{cen} have polynomial n-dependence properties similar to the general loop system if ρ_{cen} is defined as the minimal distance of the source point from the axial boundary points $(Z_{\min}(R), R)$ and $(Z_{\max}(R), R)$ of the analytical integrals in these formulas. Therefore, in these special cases, the central convergence region should be defined by the effective central convergence radius introduced in Section 2 (Eq. (13)).

With the above convergence radius definitions, the source constants usually vary slowly with n (in most cases they decrease with n), and the rate of convergence of the series depends mainly on the convergence ratio $\mathcal{R}_c = x$. Table 1 shows, with a few examples, the connection between the convergence rate and $\mathcal{R}_c$: one can see there the number of non-zero terms N in the field series that are necessary to get a relative accuracy of 10^{-12} for the magnetic field, for various magnetic systems, source points and field points. To get the relative accuracy values of the zonal harmonic series results, we compared them with field values computed with elliptic integrals; the latter have in our codes double precision (10^{-15}) accuracy. The second row of Table 1 gives the number of terms for the simple geometrical series, corresponding to $c_n = 1$ constant coefficients. The central series for 1 current loop has a similar convergence rate as the geometrical series; the absolute values of the source constants here increase with $\sqrt{n}$. In the case of 5000 loops, with cylindrical geometry and with source point outside the cylinder, the source constant absolute values decrease slightly with n (e.g., $B_{5000}^{cen}/B_0^{cen} = 0.07$, $B_{5000}^{rem}/B_2^{cen} = -0.2$), and the convergence rate is slightly higher. For the central series the situation is completely different when the source point is inside the

cylinder of the 5000 loops: then the central source constants decrease rapidly with n (e.g., $B_{10}^{cen}/B_0^{cen} \sim 10^{-7}$, $B_{30}^{cen}/B_0^{cen} \sim 10^{-17}$), and due to this rapid decrease the convergence here is extremely fast. We mention that the n-dependence of the central source constants in this case is due to cancellation effects among the sinusoidally oscillating Legendre polynomials (compare with Section 6 of Ref. [32]). The case of the 5000 loops with cylindrical geometry is similar to the case of a coil where the minimal central convergence radius is used instead of the effective one. The coil examples in Table 1 use the effective central convergence radius for the convergence ratio definition, therefore the numbers N with $z_0 = 0$ (source point at center of coil) are much higher. Note that the $\mathcal{R}_c = 0.99$, $z_0 = 0$, $u = 0$ field point has $r = 4.02$ radius value, i.e., it is far outside the coil. We mention also that in the case of $z_0 = 0$ all the source constants of odd n are zero, therefore the maximal indices n of the series used in these calculations are about two times larger than the number of non-zero terms given in Table 1.

Table 1. Number of non-zero zonal harmonic terms N that are necessary to get a relative precision of 10^{-12} for magnetic field of loops, coil and magnetically charged disk, for various convergence ratios $\mathcal{R}_c = \rho/\rho_{cen}$ (central) or $\mathcal{R}_c = \rho_{rem}/\rho$ (remote), and for various source point coordinates z_0. First row: geometrical series $1 + x + x^2 \ldots$, for comparison. 1 loop: axial coordinate $Z = 0$, radius $R = 1$. 5000 loops: equidistant loops between $Z_{\min} = -4$ and $Z_{\max} = 4$, all loops have the same radius ($R = 1$) and the same current. Coil: $Z_{\min} = -4$, $Z_{\max} = 4$, $R_{\min} = 0.7$, $R_{\max} = 1$, constant current density; for $z_0 = 0$: $\rho_{cen}^{\min} = 0.7$, $\rho_{cen}^{eff} = 4.06$, $\rho_{rem} = 4.12$. Disk: end disk of the above coil at $Z = Z_{\max} = 4$. Field point direction in all cases: $u = \cos\theta = 0$, except for disk $u = 0.5$. SI units are used.

$\mathcal{R}_c$	0.1	0.5	0.7	0.9	0.95	0.98	0.99
Geometrical series	13	40	78	263	539	1368	2750
1 loop, central, $z_0 = 1$	10	36	72	244	504	1280	2576
5000 loops, central, $z_0 = 5$	10	34	66	206	410	1026	2003
5000 loops, central, $z_0 = 1$	4	10	14	18	18	18	18
Coil, central, $z_0 = 4$	7	27	53	173	339	899	1719
Coil, central, $z_0 = 0$	5	16	32	88	188	433	741
Coil, remote, $z_0 = 0$	6	19	35	100	183	433	773
Disk, remote, $z_0 = Z_{\max} = 4$	6	16	28	88	169	385	709

Table 2. Number $N(J)$ and $N(\sigma_m)$ of non-zero central and remote zonal harmonic terms that are necessary to get a relative precision of 10^{-12} field accuracy for the coil defined at Table 1. Comparison of the current method ($N(J)$, Section 4) and the magnetic charge method ($N(\sigma_m)$, end of Section 6), for various field points with cylindrical coordinates $z = 0$ and r. For the current method the source point $z_0 = 0$ (center of coil) is used. $\mathcal{R}_c(J)$ denotes the central (first 5 values) or remote (last 5 values) convergence ratio for the current method (the 1.01 value is a common central and remote convergence ratio); $\mathcal{R}_c(\sigma_m)$ is the remote convergence ratio for the magnetic charge method.

r	0.81	2.44	3.45	3.86	4.02	4.09	4.16	4.34	4.85	6.87	20.62
$\mathcal{R}_c(J)$	0.2	0.6	0.85	0.95	0.99	1.01	0.99	0.95	0.85	0.6	0.2
$\mathcal{R}_c(\sigma_m)$	0.25	0.21	0.19	0.18	0.18	0.18	0.17	0.17	0.16	0.13	0.05
$N(J)$	8	24	62	189	742	-	773	183	61	25	8
$N(\sigma_m)$	16	16	16	14	14	14	14	14	14	12	10

Table 2 provides a comparison of the rate of convergence for the current and magnetic charge methods. Again, $N(J)$ and $N(\sigma_m)$ are the number of non-zero terms in the zonal harmonic series that are needed to get 10^{-12} relative accuracy for the magnetic field B of the coil defined in Table 1, for various field points at the mirror symmetry plane of the coil. The first 5 field points are inside the effective central convergence region of the coil, and the last 5 field points are inside the remote convergence region of the coil. Convergence ratio values $\mathcal{R}_c(J)$ close to 1 result in a large number of terms $N(J)$ in the central or remote series; at the 6th field point both the central and remote convergence ratio of the current method is 1.01, so neither the central nor the remote series can be used here. On the other hand, the remote convergence ratio values $\mathcal{R}_c(\sigma_m)$ of the magnetic charge method are at all the 11 field points rather small (around 0.2), so this method has, at these points, high rate of convergence. In general, one can say first that for all coils there exists a circular band region where both the central and the remote series of the current method are divergent, but in a large part of this region the magnetic charge method is convergent. And second, there exist two circular band regions where the convergence of the zonal harmonic expansions with the magnetic charge method is faster than with the current method.

At the end of this section, we present some computation time comparisons between the elliptic integral and the zonal harmonic methods. First, in the case of 1 current loop, the field computation

times of these two methods are quite similar; in fact, the elliptic integral method is in this special case somewhat faster. For example, with our notebook (multiplication time: 0.5 ns) the elliptic integral field calculation time is about 2 μs, and for $\mathcal{R}_c = 0.2$, 0.5 and 0.8 values with the zonal harmonic method we have 1.5, 3 and 10 μs CPU times, respectively. The situation is quite different if we have many loops. Namely, the field computation time with the elliptic integral method is proportional to the number of loops, and the same proportionality is valid for the source constant calculations. On the other hand, the field calculation time with the zonal harmonic method is independent of the number of loops, it depends only on the convergence ratio. Similarly, in the case of the coil of Table 1 the elliptic integral method time is much larger than for 1 loop (about 300 μs), but the zonal harmonic method time values are similar to the case of the loop: with $\mathcal{R}_c = 0.5$, 0.8 and 0.98 we have 1.3, 3 and 20 μs CPU times, respectively. We can see here also that for the same $\mathcal{R}_c$ value the zonal harmonic method for the coil is somewhat faster than for the loop: this is due to the different n-dependence of the source constants.

8. THREE-DIMENSIONAL MAGNETIC SYSTEMS

The axisymmetric field calculation method described so far can be extended to a three-dimensional magnetic system where each component (coil or magnetic material) is axisymmetric within its own local coordinate system. For the sake of simplicity, we shall assume in the present section that the magnetic system contains only coils (nevertheless, our considerations are equally valid for magnetic materials). One divides the system into symmetry groups, so that all coils belonging to one of the symmetry groups have the same symmetry axis. The zonal harmonic method can be used separately for each symmetry group, with coil geometry, source points, source constants, cylindrical coordinates and field components defined within the local coordinate systems, and then the magnetic field in the global system can be computed as the sum of the field contributions from the symmetry groups, using some appropriate coordinate transformations.

The first task in this procedure is the division of the coils into symmetry groups. Let us assume that we have coils with rectangular cross section, and the two center points of the end disks of coil i are given in the global coordinate system by the position vectors $\mathbf{X}_i$ and $\mathbf{Y}_i$. We define for coil 1 the point $\mathbf{X}_1$ as the origin of a local coordinate system ($\mathbf{P}_0 = \mathbf{X}_1$), and the unit direction vector $\mathbf{u} = (\mathbf{Y}_1 - \mathbf{X}_1)/|\mathbf{Y}_1 - \mathbf{X}_1|$ should determine the local symmetry axis of the symmetry group number 1. Then one has to find all the other

coils (in addition to coil 1) that belong also to this symmetry group. For example, coil 2 is in this symmetry group if and only if its both end points $\mathbf{X}_2$ and $\mathbf{Y}_2$ are on the previously defined symmetry axis. Defining the unit vector $\mathbf{x} = (\mathbf{X}_2 - \mathbf{X}_1)/|\mathbf{X}_2 - \mathbf{X}_1|$, we can see that the point $\mathbf{X}_2$ is practically on this axis if either $|\mathbf{u} - \mathbf{x}| < \varepsilon$ or $|\mathbf{u} + \mathbf{x}| < \varepsilon$, where ε is some small tolerance number (for example: $\varepsilon = 10^{-8}$). We make a similar test for the other end point of coil 2 ($\mathbf{Y}_2$), and then these tests for all the other coils. We repeat this group searching procedure until for each coil in the system a symmetry group has been found. One possible outcome of this searching can be that all coils belong to the same symmetry group: in this case we have a fully axisymmetric system, although its symmetry axis could be different from the z axis of the global coordinate system. It can also happen that the number of symmetry groups is equal to the number of coils; this is the worst case, from the point of view of computation time with the zonal harmonic expansion method.

Once we have found the symmetry groups, we have to determine first the local axial end point coordinates of the coils; for example, coil 1 in the above example has $Z_{\min}^{loc} = 0$ and $Z_{\max}^{loc} = |\mathbf{Y}_1 - \mathbf{X}_1|$. The signs of the current densities in the local cordinate systems should also be determined. Then, we define the local central and remote source points along the symmetry axes, and we compute the corresponding source constants.

Let us now consider a field point $\mathbf{P}$, whose components are defined in the global coordinate system, and let us calculate at this point the magnetic field contribution $\mathbf{B}$ due to the coils belonging to the symmetry group that has the origin point $\mathbf{P}_0$ and axial unit direction vector $\mathbf{u}$. The local cylindrical coordinates of point $\mathbf{P}$ are

$$z_{loc} = (\mathbf{P} - \mathbf{P}_0) \cdot \mathbf{u}, \quad r_{loc} = |\mathbf{r}_{loc}|, \quad \mathbf{r}_{loc} = \mathbf{P} - \mathbf{P}_0 - z_{loc}\mathbf{u}. \quad (54)$$

Using the axisymmetric zonal harmonic expansions described in the previous sections, with z and r substituted for z_{loc} and r_{loc}, we can calculate the local cylindrical field components B_z^{loc} and B_r^{loc}, and we obtain the magnetic field contribution of the symmetry group in the global system as

$$\mathbf{B} = B_z^{loc}\,\mathbf{u} + B_r^{loc}\,\mathbf{v}, \quad \mathbf{v} = \mathbf{r}_{loc}/r_{loc}. \quad (55)$$

9. MAGNETIC FIELD COMPUTATION IN PRACTICE

In order to apply the zonal harmonic method for field calculation of a magnetic system, the first step is to find the sources (currents and magnetization) of the field. In the case of coils this is trivial: the currents or current densities of the coils are usually known input

parameters. Similarly, the magnetization of permanent magnets is also known. In case of magnetic materials with induced (soft) magnetization, this has to be computed using some appropriate integral equation or finite element method [3, 19].

The second step is to find the symmetry groups of the system. Then, for each symmetry group, one defines several central source points along the local symmetry axis. They should be chosen so that the central zonal harmonic expansion should be convergent within a large region inside and near the local magnetic system. For example, the optimal distance between two neighboring central source points should be a few times smaller than the central convergence radius at these points; otherwise, it could happen that the central zonal method is not convergent at some points near the axis. Next, one defines remote source points at the center of the symmetry group, at the center of each component (coil or magnetic material) of the group, and at the two center points of the end disks of coils with rectangular cross section (the latter are necessary in order to apply the magnetic charge method discussed in Section 6). Using the remote source points, we can compute the field far from the group, and also in regions near and within the group where the central expansion method is not convergent. Far from the group and near the axis one could also use the central expansion method; nevertheless, for this purpose one would have to define many central source points far away from the group, and this would increase the source constant and source point searching (see below) computation time.

After the source points have been defined, the code should compute the source constants at all these points. The maximal source constant index n_{max} should be chosen a few hundred or 1000, depending on the requirements of the convergence ratio and of the accuracy of the field computation (see Table 1). The source constant computation time is proportional to n_{max}, but this is typically only a minute or less, and the source constants have to be calculated only once for a fixed magnetic system configuration. In addition to the source constants, also the convergence radii for all source points have to be computed. At the end, the source points, convergence radii and source constants for all symmetry groups are saved to the hard disk, so that they could be used for field computation later.

The magnetic field at a field point is the sum of field contributions from all symmetry groups. To apply the fast zonal harmonic method for the field computation of a group, the computer code has to find in this group a central or remote source point for which the zonal harmonic expansion is convergent. Moreover, to minimize the computation time, the code should find the best source point, with a

minimal number of terms in the series to get a prescribed accuracy level for the field. This is usually the source point which has the smallest convergence ratio for the actual field point. In case of mirror symmetry of the group, the source point at the center of the group has the advantage that only the even-n source constants are non-zero. If the field point is far from the group, the code should choose the remote source point at the center of the group: fast convergence is then guaranteed. For field points inside the group and with many central source points the searching procedure could take some time. One possibility to reduce this time during trajectory calculations is to restrict the searching for those central source points that are near the best source point found in the previous trajectory step. In some rare cases, it can happen that for the actual field point no source point with satisfactory convergence properties can be found. In this case, elliptic integrals have to be used for the field calculation of the symmetry group.

An important practical question is the truncation criterion for the zonal harmonic series: at which index n should one stop the expansions, in order to get some prescribed accuracy? In our codes, to get double precision accuracy for the field components, we use the following procedure: the field components B_z and B_r are computed together, using the same Legendre polynomial evaluations, and the expansion is stopped if the sum of the absolute values of the last 4 terms in the series of the field components are 10^{15} times smaller than the $|B_z| + |B_r|$ sum of the corresponding series, or if the $|B_z| + |B_r|$ value is smaller than some small, user-defined number. A similar (but slightly different) truncation criterion was suggested by Garrett in Refs. [24, 25].

At the end of this section, we present a few computation time examples for magnetic field calculations of the KATRIN experiment [17]. First, we computed the magnetic field of the 17 coils near the KATRIN main spectrometer, all coils having the z axis as symmetry axis. The computation time of 90000 central source constants at 140 source points ($n_{\max} = 500$) is with our notebook (multiplication time: 0.5 ns) about 3 s. The field computation of the 17 coils with elliptic integrals takes 2.5 ms, and with zonal harmonic expansions at field points with convergence ratios of 0.5 and 0.8 the CPU times are 2 μs and 5 μs, respectively. Then, we computed the magnetic field of 62 coils of the KATRIN experiment, with 7 symmetry groups. The source constant computation time in this case is 200 s, the field computation time with elliptic integrals at points inside the KATRIN main spectrometer is 7 ms, and with zonal harmonic expansions at field points with convergence ratios of 0.5 and 0.8 the

computation times are 6 μs and 10 μs, respectively. These examples illustrate also (in addition to Section 7) that the zonal harmonic expansion magnetic field calculation method is by several orders of magnitude faster than the elliptic integral method.

10. CONCLUSION

We have presented in this paper the central and remote zonal harmonic expansion method for magnetic field calculations of axially symmetric coil and magnetic material systems. The zonal harmonic field series formulas are convergent at field points within the central and remote regions, which have spherical boundaries, and their center, the source point, can be arbitrarily chosen on the symmetry axis. The rate of convergence of the field series depends on the distance of the field and the source point; smaller distance for central field points and larger distance for remote field points correspond to higher convergence rate. For a given field point, one can improve the convergence properties of the zonal harmonic method by optimal choice of the field expansion method (central or remote), of the source point, and of the magnetic source representation method (current, magnetic material, or magnetic charge). In order to use the zonal harmonic formulas for field calculations, one needs the source constants, which depend on the source point and on the geometrical and source strength properties of the magnetic system. In our paper, we have presented source constant computation formulas for circular current loops, for general axisymmetric coils, for axisymmetric magnetic materials, and for special coils having rectangular cross section and current density that is independent of the axial coordinate. We have also shown that the zonal harmonic method is applicable for special three-dimensional magnetic systems, whose components (coils or magnetic materials) are axially symmetric in their own local coordinate systems.

We have made many computations and comparisons with published results to test our zonal harmonic expansion method:

- Circular loops and thick coils (with rectangular cross section and constant current density): comparison of the field at various points with elliptic integral calculations; close to double precision agreement was found in all cases (compare with Section 7). Comparisons of magnetic field computations of the current method with the magnetic charge method.

- Magnetic materials: comparison with dipole integration and with various elliptic integral calculations (see Section 5).

- Comparison with the analytical on-axis field of the thick coil (with rectangular cross section and constant current

density) [4, 30, 67, 68]; we compared also the analytical expressions for the higher derivatives of this on-axis field with the central zonal harmonic derivatives.

- Comparisons of our zonal harmonic formulas with Refs. [23–25, 64, 65].
- Comparisons of our elliptic integral formulas with Refs. [19, 21, 27].

The zonal harmonic magnetic field calculation method has several important advantages.   First, the field and source equations are separated: during the source constant computations one has to use only the source point and source parameters (geometry, currents, magnetization), but not the field point parameters; and during the field computation the source constants contain already the whole information about the magnetic sources. As an important consequence, the magnetic field calculation with the zonal harmonic method is much faster (in some cases even 1000 times) than with the widely known elliptic integral method. Second, the zonal harmonic method has not only high speed, but also high accuracy, which makes the method especially appropriate for trajectory calculations of charged particles. Due to these properties, no interpolation is necessary when the magnetic field during particle trajectories is computed with the aid of the zonal harmonic method.   Third, it is more general and for practical applications more advantageous than the radial series expansion method, which is more widely known in the electron optics literature than the zonal harmonic method.   In addition, the zonal harmonic field series formulas are relatively easy to differentiate and integrate, in contrast to the elliptic integral formulas. Furthermore, the low-order source constants can be helpful for system design optimization; for example, vanishing low-order central source constants imply a homogenous magnetic field near the central source point.

The axisymmetric zonal harmonic method could be generalized to spherical harmonic method, for magnetic field calculation of general three-dimensional systems.   In that case, we have two-dimensional spherical harmonic expansions, instead of the one dimensional zonal harmonic expansions.   The source point can then be an arbitrary point in space (not restricted to any symmetry axis), and the central and remote convergence radii are, similarly to the zonal harmonic method, the minimal and maximal distances of the source point from the magnetic sources, respectively. Due to the two-dimensionality of the series, this three-dimensional method is probably fast enough only for convergence ratios that are much smaller than 1.

ACKNOWLEDGMENT

REFERENCES

1. Paszkowski, B., *Electron Optics*, London Eliffe Books, New York American Elsevier, 1968.

2. Szilágyi, M., *Electron and Ion Optics*, Plenum Press, New York and London, 1988.

3. Hawkes, P. W. and E. Kasper, *Principles of Electron Optics*, Vol. 1, Academic Press, Harcourt Brace Jovanovich, 1989.

4. Montgomery, D. B. and R. J. Weggel, *Solenoid Magnet Design*, Robert E. Krieger Publ. Comp., New York, 1980.

5. Saint-Jalmes, H., J. Taquin, and Y. Barjhoux, "Optimization of homogeneous electromagnetic coil systems: Application to whole-body NMR imaging magnets," *Rev. Sci. Instrum.*, Vol. 52, 1501, 1981.

6. Williams, J. E. C., "Superconducting magnets for MRI," *IEEE Trans. Nucl. Sci.*, Vol. 31, 994, 1984.

7. Sanger, P. A., "Present status of MRI magnets at Oxford," *IEEE Trans. Magnetics*, Vol. 21, 436, 1985.

8. Morad, R., et al., "Way of improving the stability and homogeneity of MRI magnets," *IEEE Trans. Magnetics*, Vol. 24, 1282, 1988.

9. Vetter, J., G. Ries, and T. Reichert, "A 4-tesla superconducting whole-body magnet for MR imaging and spectroscopy," *IEEE Trans. Magnetics*, Vol. 24, 1285, 1988.

10. Shimada, Y., et al., "Superconducting magnet with self-shield for whole body magnetic resonance imaging," *IEEE Trans. Magnetics*, Vol. 27, 1685, 1991.

11. Kraus, C., et al., "Final results from phase II of the Mainz neutrino mass search in tritium β decay," *Eur. Phys. J. C*, Vol. 40, 447, 2005.

12. Lobashev, V. M., "The search for the neutrino mass by direct method in the tritium beta-decay and perspectives of study it in the project KATRIN," *Nucl. Phys. A*, Vol. 719, 153c, 2003.

13. Glück, F., et al., "The neutron decay retardation spectrometer aSPECT: Electromagnetic design and systematic effects," *Eur. Phys. J. A*, Vol. 23, 135, 2005.

14. Baessler, S., et al., "First measurements with the neutron decay spectrometer aSPECT" *Eur. Phys. J. A*, Vol. 38, 17, 2008.

15. Beck, M., et al., "WITCH: A recoil spectrometer for weak interaction and nuclear physics studies," *Nucl. Instrum. Methods A*, Vol. 503, 567, 2003.

16. Friedag, P., "Bahnverfolgungssimulationen für das WITCH experiment," Diploma thesis, University of Münster, 2008.

17. Angrik, J., et al., "KATRIN design report 2004," FZKA Scientific Report 7090, Forschungszentrum Karlsruhe, 2005, http://bibliothek.fzk.de/zb/berichte/FZKA7090.pdf.

18. Maxwell, J. C., *A Treatise on Electricity and Magnetism*, Vol. 1, Clarendon Press, 1873.

19. Durand, E., *Magnetostatique*, Masson et Cie, Editeurs, Paris, 1968.

20. Jackson, J. D., *Classical Electrodynamics*, John Wiley & Sons, New York, 1999.

21. Smythe, W. R., *Static and Dynamic Electricity*, McGraw Hill Book Company, New York, 1968.

22. Kellogg, O. D., *Foundations of Potential Theory*, Springer Verlag, Berlin, 1967.

23. Garrett, M. W., "Axially symmetric systems for generating and measuring magnetic fields," *J. Appl. Phys.*, Vol. 22, 1091, 1951.

24. Garrett, M. W., "The method of zonal harmonics," *High Magnetic Fields*, H. Kolm, et al. (eds.), John Wiley and Sons, 1962.

25. Garrett, M. W., "Computer programs using zonal harmonics for magnetic properties of current systems with special reference to the IBM 7090," ORNL-3318, Oak Ridge National Laboratory, USA, 1962.

26. Garrett, M. W., "Thick cylindrical coil systems for strong magnetic fields with field or gradient homogeneities of the 6th to 20th order," *J. Appl. Phys.*, Vol. 38, 2563, 1967.

27. Garrett, M. W., "Calculation of fields, forces, and mutual inductances of current systems by elliptic integrals," *J. Appl. Phys.*, Vol. 34, 2567, 1963.

28. Franzen, W., "Generation of uniform magnetic fields by means of air-core coils," *Rev. Sci. Instrum.*, Vol. 33, 933, 1962.

29. Marshall, H. L. and H. E. Weaver, "Application of the Garrett method to calculation of coil geometries for generating homogeneous magnetic fields in superconducting solenoids," *J. Appl. Phys.*, Vol. 34, 3175, 1963.

30. Girard, B. and M. Sauzade, "Calcul des solenoides compenses du 6eme ordre a volume de bobinage minimum," *Nucl. Instrum. Methods*, Vol. 25, 269, 1964.

31. Kaminishi, K. and S. Nawata, "Practical method of improving the uniformity of magnetic fields generated by single and double Helmholtz coils," *Rev. Sci. Instrum.*, Vol. 52, 447, 1981.

32. Glück, F., "Axisymmetric electric field calculation with zonal harmonic expansion," *Progress In Electromagnetics Research B*, Vol. 32, 319–350, 2011.

33. Flatt, B., "Designstudien für das KATRIN Experiment," Diploma thesis, University of Mainz, 2001.

34. Thümmler, T., "Entwicklung von Methoden zur Untergrundreduzierung am Mainzer Tritium-β-Spektrometer," Diploma thesis, University of Mainz, 2002.

35. Müller, B., "Umbau des Mainzer Neutrinomassenexperiments und Untergrunduntersuchungen im Hinblick auf KATRIN," Diploma thesis, University of Mainz, 2002.

36. Essig, K., "Untersuchungen zur Penningfalle zwischen den Spektrometern des KATRIN Experiments," Diploma thesis, University of Bonn, 2004.

37. Thümmler, T., "Präzisionsüberwachung und Kalibration der Hochspannung für das KATRIN Experiment," Dissertation, University of Münster, 2007.

38. Pocanic, D., et al., "Nab: Measurement principles, apparatus and uncertainties," *Nucl. Instrum. Methods A*, Vol. 611, 211, 2009.

39. Dubbers, D., et al., "A clean, bright, and versatile source of neutron decay products," *Nucl. Instrum. Methods A*, Vol. 596, 238, 2008.

40. Valerius, K., "Elektromagnetisches Design für das Hauptspektrometer des KATRIN Experiments," Diploma thesis, University of Bonn, 2004.

41. Valerius, K. "Spectrometer-related background processes and their suppression in the KATRIN experiment," Dissertation, University of Münster, 2009.

42. Hugenberg, K., "Design of the electrode system for the KATRIN main spectrometer," Diploma thesis, University of Münster, 2008.

43. Zacher, M., "Electromagnetic design and field emission studies for the inner electrode system of the KATRIN main spectrometer," Diploma thesis, University of Münster, 2009.

44. Wandkowsky, N., "Design and background simulations for the KATRIN main spectrometer and air coil system," Diploma thesis, Karlsruhe Institute of Technology, 2009.

45. Fränkle, F., "Background investigations of the KATRIN Pre-spectrometer," Dissertation, Karlsruhe Institute of Technology, 2010.

46. Sturm, M., "Bestimmung der Tritiumflussreduktion einer Tritium-Argon-Frostpumpe für das Neutrinomassenexperiment KATRIN," Diploma thesis, Karlsruhe Institute of Technology, 2007.

47. Groh, S., "Untersuchung von UV-Laser induziertem Untergrund am KATRIN Vorspektrometer," Diploma thesis, Karlsruhe Institute of Technology, 2010.

48. Reimer, S., "Ein elektrostatisches Dipolsystem zur Eliminierung von Ionen in der DPS2-F des KATRIN Experimentes," Diploma thesis, Karlsruhe Institute of Technology, 2009.

49. Hötzel, M., "Berechnung von KATRIN Messspektren unter Einbeziehung der Eigenschaften der fensterlosen gasförmigen Tritiumquelle," Diploma thesis, Karlsruhe Institute of Technology, 2009.

50. Schwarz, J., "Design zur Messung der elektro-optischen Eigenschaften der differentiellen Pumpstrecke DPS2-F des KATRIN Experiments," Diploma thesis, Karlsruhe Institute of Technology, 2010.

51. Valerius, K., et al., "Prototype of an angular-selective photoelectron calibration source for the KATRIN-experiment," *J. Inst.*, Vol. 6, P01002, 2011.

52. Lukic, S., et al., "Ion source for tests of ion behavior in the KATRIN beam line," *Rev. Sci. Instrum.*, Vol. 82, 013303, 2011.

53. KATRIN homepage, Talks and Publications, Diploma and Ph.D. theses, http://www-ik.fzk.de/~katrin/publications/thesis.html.

54. Westfälische Wilhelms-Universität Münster, Institut für Kernphysik, AG Prof. Dr. C. Weinheimer, http://www.uni-muenster.de/Physik.KP/AGWeinheimer/Arbeiten-de.html.

55. Vöcking, S., "Implementierung der multipole boundary element methode für das KATRIN-experiment," Diploma thesis, University of Münster, 2008.

56. Corona, T. J., "Tools for electromagnetic field simulation in the KATRIN experiment," Master thesis, MIT, 2009.

57. Leiber, B., "Non-axially symmetric field and trajectory calculations for the KATRIN experiment," Diploma thesis, Karlsruhe Institute of Technology, 2010.

58. Babutzka, M., et al., *The Comprehensive Guide to KASSIOPEIA*, Version 1.00.00, KATRIN internal report.

59. Cowan, E. W., *Basic Electromagnetism*, Academic Press, New York, 1968.

60. Panofsky, W. K. H. and M. Phillips, *Classical Electricity and Magnetism*, Dover Publications, Mineola, New York, 1962.

61. Wangsness, R. K., *Electromagnetic Fields*, John Wiley & Sons, New York, 1979.

62. Ravaud, R., G. Lemarquand, V. Lemarquand, and C. Depollier, "Discussion about the analytical calculation of the magnetic field created by permanent magnets," *Progress In Electromagnetics Research B*, Vol. 11, 281–297, 2009.

63. Ravaud, R. and G. Lemarqand, "Comparison of the Coulombian and Amperian current models for calculating the magnetic field produced by radially magnetized arc-shaped permanent magnets," *Progress In Electromagnetics Research*, Vol. 95, 309, 2009.

64. Zisserman, A., R. Saunders, and J. Caldwell, "Analytic solutions for axisymmetric magnetostatic systems involving iron," *IEEE Trans. Magnetics*, Vol. 23, 3895, 1987.

65. Saunders, R., A. Zisserman, and C. J. McCauley, "The calculation of magnetostatic fields from axisymmetric conductors," *J. Phys. D*, Vol. 29, 533, 1996.

66. Ravaud, R., et al., "Mutual inductance and force exerted between thick coils," *Progress In Electromagnetics Research*, Vol. 102, 367, 2010.

67. Gardner, M. E., et al., "Production of a uniform magnetic field by means of an end-corrected solenoid," *Rev. Sci. Instrum.*, Vol. 31, 929, 1960.

68. Andrew, E. R., I. Roberts, and R. C. Gupta, "Helmholtz-type coils of finite cross section," *J. Sci. Instrum.*, Vol. 43, 936, 1966.